

## Preparation of Anionic Ion Exchange Latex Particles via Heteroaggregation

Su Jeong Han,<sup>1,2</sup> Eric S. Daniels,<sup>1</sup> E. David Sudol,<sup>1</sup> Victoria L. Dimonie,<sup>1</sup> Andrew Klein<sup>1,2</sup>

<sup>1</sup>Emulsion Polymers Institute, Lehigh University, Bethlehem, Pennsylvania 18015

<sup>2</sup>Department of Chemical Engineering, Lehigh University, Bethlehem, Pennsylvania 18015

Correspondence to: E. S. Daniels (E-mail: eric.daniels@lehigh.edu)

**ABSTRACT:** To prepare relatively large negatively charged polymer particles in a size range from 0.3  $\mu\text{m}$  to 0.5  $\mu\text{m}$ , having high surface charge densities, the heteroaggregation of small (50–100 nm), highly charged (185 and 421  $\mu\text{eq/g}$ ) anionic polystyrene particles onto the surface of larger (317–466 nm) poly(vinylbenzyl chloride)-based cationic (10, 614, and 830  $\mu\text{eq/g}$ ) particles was carried out. As a result, particles with different surface charges, having a core-shell structure, were successfully prepared. First, aggregated particles were formed via heteroaggregation of the lowest surface charge density anionic particles (185  $\mu\text{eq/g}$ ) with the lowest surface charge density cationic particles (10  $\mu\text{eq/g}$ ). However, the anionic particles in the shell layer desorbed with time owing to the relatively weak interaction between the two particles. Second, aggregated particles comprised of the highest surface charge density cationic (830  $\mu\text{eq/g}$ ) and anionic latex particles (421  $\mu\text{eq/g}$ ) were formed. However, to prepare a stable system, an excess of the small anionic particles was required, leaving a large number of small particles present in the aqueous phase, which proved difficult to remove. Finally, aggregated particles were formed by heteroaggregation of cationic particles with an intermediate surface charge density (614  $\mu\text{eq/g}$ ) with the highest surface charge anionic particles (421  $\mu\text{eq/g}$ ). As a result, not only were core-shell particles formed, but few free small anionic particles remained in the aqueous phase. In this article, the preparation and characterization of each of these aggregates are discussed in terms of particle size, morphology, and extent of incorporation of the functional groups.  
© 2012 Wiley Periodicals, Inc. *J. Appl. Polym. Sci.* 000: 000–000, 2012

**KEYWORDS:** colloids; core/shell polymers; emulsion polymerization; functionalization of polymers; heteroaggregation

Received 8 December 2011; accepted 24 March 2012; published online

**DOI:** 10.1002/app.37798

### INTRODUCTION

Polymer particles with various functional groups present on the surface have extensive applications in a variety of fields such as inks<sup>1</sup> and coatings,<sup>2</sup> protein synthesis,<sup>3</sup> and biomedical applications.<sup>4</sup> Among these, a great deal of research has involved the preparation of polystyrene sulfonic acid ion exchange resins for various applications. For example, one application used sulfonic acid ion exchange resin as a catalyst to obtain a certain molecular weight polymer.<sup>5,6</sup> Separation of the transition metal complex catalyst from the polymer in ATRP (atom transfer radical polymerization) is another frequently used application of sulfonic acid ion exchange resin as it is more cost effective than other separation methods using an alumina column, precipitation of polymer in a non-solvent, or precipitation of Cu complex with NaOH or Na<sub>2</sub>S, in the sense that repeated precipitations require the use of significant amounts of solvent.<sup>7,8</sup> Also, one researcher reported that magnetic nanoparticles ( $\gamma\text{-Fe}_2\text{O}_3$ ),<sup>9</sup>

which are attractive for many applications such as magnetic recording,<sup>10</sup> ceramics,<sup>11</sup> drug delivery,<sup>12</sup> magnetic resonance imaging (MRI) in medical diagnosis,<sup>13–17</sup> and magnetic field induced excitation for cancer therapy,<sup>18–20</sup> could be embedded in a polymer matrix via ion exchange. In this method, ion exchange resin, having  $\text{SO}_3^- \text{H}^+$  groups present, was exchanged with  $\text{Fe}^{2+}$  ions from an aqueous solution of ferrous sulfate followed by thorough washing to remove excess  $\text{Fe}^{2+}$  ions. These exchanged  $\text{Fe}^{2+}$  ions were then converted into  $\text{Fe}(\text{OH})_2$  by the addition of NaOH solution, followed by adding dilute solution of  $\text{H}_2\text{O}_2$  to obtain  $\gamma\text{-Fe}_2\text{O}_3$  as a final product. More recently, research has focused on the proton-conducting components in PEM (proton-exchange membrane) fuel cells.<sup>21–23</sup> Substitutes have been prepared for Nafian<sup>®</sup> (DuPont),<sup>24</sup> a perfluorosulfonic acid polymer, which is commercially available, but at a high cost. In addition, there are environmental hazards associated with its disposal due to the fluorine content, with different polymers.

Sulfonated polymers combined with crosslinked polystyrene sulfonate ion exchange resin, where the presence of sulfonate groups enables fast transport which is a crucial feature in fuel cell applications.

In this study, sulfonated polystyrene latex particles are being developed for application in fluids where it is important to maintain low conductivity. A great deal of research has been carried out to prepare sulfonated polystyrene latex particles using sodium styrene sulfonate (NaSS).<sup>25–28</sup> However, most of these polystyrene-based particles were either only lightly sulfonated with a low surface charge density, or their final particle size was small. Particles with high surface charge densities ( $>200 \mu\text{eq/g}$ ) are usually synthesized by adding increasing amounts of functional comonomer. This normally results in a decrease in particle size in conventional emulsion polymerization and would result in an increase in conductivity particularly for particles smaller than  $100 \text{ nm}$ <sup>29</sup> which is not suitable for our given application. On the other hand, the conductivity is low when using larger size latex particles. However, these larger particles typically have a much lower concentration of total bound and surface-bound functional groups compared to the smaller particle diameter latexes.<sup>30</sup> Thus, preparing large anionic latex particles with high surface charge densities is a major challenge as mentioned earlier. In this article, a heteroaggregation technique<sup>31,32</sup> is applied to meet the challenges outlined above, to obtain large, highly charged particles without significantly affecting the latex conductivity. Heteroaggregation is defined as the aggregation of colloidal particles that may differ in charge,<sup>33–35</sup> size,<sup>36,37</sup> or both.<sup>38</sup> Thus, this technique was explored by preparing small ( $\sim 50\text{--}100 \text{ nm}$ ), highly charged ( $200\text{--}500 \mu\text{eq/g}$ ), anionic particles varying in size and charge and heteroaggregating them by electrostatic interactions,<sup>39</sup> or hydrogen bonding interactions<sup>40,41</sup> onto larger cationic particles ( $>300 \text{ nm}$ ), also varying in size and charge. The development of this aggregation method and the subsequent stabilization of the resulting heteroaggregated system are described in this article. The latter includes investigation of the type and concentration of stabilizer and the effect of the solvency of the medium on the process.

## EXPERIMENTAL

### Materials

Styrene (St, Sigma-Aldrich) monomer was distilled in the presence of cuprous chloride at a reduced pressure of  $35 \text{ mmHg}$  at  $55^\circ\text{C}$  to remove inhibitor and any oligomers. Vinylbenzyl chloride (VBC, Sigma-Aldrich), divinylbenzene crosslinking monomer (DVB 80, Dow Chemical), vinylbenzyl trimethylammonium chloride (VBTMAC, Sigma-Aldrich), and sodium styrene sulfonate (NaSS, Sigma-Aldrich) were used as received. Sodium dihexyl sulfosuccinate (Aerosol MA 80, Cytec), sodium lauryl sulfate (SLS, Sigma-Aldrich), poly(1-vinyl-2-pyrrolidone; PVP K-30, MW =  $40,000 \text{ g/mol}$  and PVP K-90, MW =  $360,000 \text{ g/mol}$ , Fluka), and polyoxyethylene (40) nonylphenyl ether (Igepal CO 880, Rhodia) were used as received without further purification. 2,2-Azobis[2-(2-imidazolin-2-yl)propane] dihydrochloride (VA-044, Wako), potassium persulfate (KPS, Sigma-Aldrich), sodium bisulfite (SBS, Sigma-Aldrich), and sodium bicarbonate

**Table I.** Recipe Used for the Preparation of Cationic Core PVBC Latex ( $\text{L}^+$ )

| Ingredient  | Amount (g)                   |
|---|------------------------------|
| Vinylbenzyl Chloride (VBC)  | 9.0                          |
| Vinylbenzyl trimethylammonium chloride (VBTMAC)                   | 0.027 (1.5 mM <sup>a</sup> ) |
| Divinylbenzene (DVB 80)   | 0.12 (1.33% <sup>a</sup> )   |
| 2,2'-Azobis[2-(2-imidazolin-2-yl)propane dihydrochloride (VA-044) | 0.09 (3.43 mM <sup>b</sup> ) |
| Deionized water (g)   | 81.0                         |

Polymerized 6 h at  $60^\circ\text{C}$ .

<sup>a</sup>On the basis of VBC., <sup>b</sup>On the basis of water.

(SBC, Sigma-Aldrich) were all used as received. Mixed-bed ion exchange resins (AG 501-X8, Bio-Rad Laboratories) were used as received without any further purification. These resins consist of an equivalent amount of cationic exchange resin ( $\text{H}^+$  form) and anionic exchange resin ( $\text{OH}^-$  form). Standardized  $0.02N$  hydrochloric acid (JT Baker) and standardized  $0.02N$  sodium hydroxide (JT Baker) were used in the conductometric titration measurements.

### Synthesis of Cationic Core Particles

Cationic core particles were prepared with three different levels of surface charge density. The two latexes with the highest charges were synthesized by modification of the lower charge latex (Table I), which was synthesized by batch emulsion polymerization in a bottle polymerizer unit. Polymerizations were carried out in 4 oz capped bottles rotated end-over-end at 32 rpm for 6 h at  $60^\circ\text{C}$ . The cationic charge was provided by the VBTMAC comonomer and VA-044 initiator. This latex, designated  $\text{L}^+$  (low positive charge), had a theoretical maximum charge of  $14.3 \mu\text{eq/g}$ .

To prepare cationic particles with higher charge density, amination of the  $\text{L}^+$  latex was carried out via reaction with trimethylamine. Thus, two sets of highly charged cationic particles were prepared by amination with two different amounts of trimethylamine, 0.60 g and 5.62 g, based on 1.6 g PVBC. The former is equivalent to a 1 : 1 ratio of amine to chloride, where the latter represents a 9 : 1 ratio. The pH of the medium was also measured, since pH is directly related to the  $\text{H}^+$  concentration, which indicates the amount of available hydrogen that can react with chloride during the amination, and not undergoing hydrolysis. The pH was 2.3 at an amine to chloride ratio of 9 : 1, giving a theoretical charge of  $\sim 5700 \mu\text{eq/g}$  if full amination would occur. These are referred to as  $\text{M}^+$  and  $\text{H}^+$  latexes (i.e., “medium” and “high” cationic charge). For both cases, trimethylamine solutions were prepared and titrated into the seed latex ( $\text{L}^+$ ) dropwise with continuous stirring using a magnetic bar in a 100 mL glass beaker at 60 rpm. Stirring was continued at room temperature for 1 day.

### Synthesis of Anionic Particles for Heteroaggregation

Two sulfonated anionic latexes were prepared with different surface charge densities (designated “low,”  $\text{L}^-$ , and “high,”  $\text{H}^-$ ).  $\text{L}^-$

**Table II.** Recipes Used to Prepare Low ( $L^-$ ) and High ( $H^-$ ) Surface Charge Anionic Latex Particles

| Ingredient                      | Amount (g) ( $L^-$ )       | Ingredient         | Amount (g) ( $H^-$ )         |
|---------------------------------|----------------------------|--------------------|------------------------------|
| Styrene (St)                    | 25.0                       | St                 | 20.0                         |
| Sodium styrene sulfonate (NaSS) | 1.0                        | NaSS               | 2.0                          |
| Divinylbenzene (DVB 80)         | 0.68 (2.7%) <sup>a</sup>   | DVB 80             | 0.04 (2.0%) <sup>a</sup>     |
| Sodium lauryl sulfate (SLS)     | 1.6 (92.5 mM) <sup>b</sup> | Aerosol MA80       | 0.75 (24.43 mM) <sup>b</sup> |
| Potassium persulfate (KPS)      | 0.1 (6.2 mM) <sup>b</sup>  | KPS                | 0.1 (4.68 mM) <sup>b</sup>   |
|                                 |                            | Sodium bicarbonate | 0.13 (19.58 mM) <sup>b</sup> |
| Deionized (DI) water            | 60.0                       | DI water           | 80.0                         |

<sup>a</sup>On the basis of styrene., <sup>b</sup>On the basis of water.

was synthesized by batch emulsion polymerization, using 4% sodium styrene sulfonate (theoretical surface charge of 186  $\mu\text{eq/g}$ ) in a 250 mL four-neck flask for 6 h at 60°C under reflux and utilizing an inert  $N_2$  atmosphere. A Teflon half-moon impeller was employed at 200 rpm. The  $H^-$  particles were prepared by bottle (batch) emulsion polymerization where the ingredients were charged to an 8 oz. bottle, purged with  $N_2$  for 2 min and then rotated end-over-end at 32 rpm in a thermostated water bath at 70°C for 24 h. Ten percentage of sodium styrene sulfonate was used as comonomer to achieve a high surface charge (theoretical surface charge of 441  $\mu\text{eq/g}$  in Table II).

#### Characterization Methods

Gravimetric analysis was used to determine the solids content of all the latexes. Dynamic light scattering (NICOMP, Model 370) was used to measure the particle diameter. The aggregated particle morphology was examined by transmission electron microscopy (TEM, Philips 400) and scanning electron microscopy (SEM, Hitachi 4300). The conductivity of the latexes was measured by a resistance conductivity probe. Differential scanning calorimetry (DSC, TA Instruments, model 2920) was used to measure the glass transition temperature ( $T_g$ ) of the polymer. The latexes were cleaned by the serum replacement technique<sup>42</sup> for 3–4 days until the conductivity of the effluent from the cell became constant and was close to the value for the deionized water supply to the cell. The latexes were then stirred with the same amount of mixed-bed ion exchange resins as the latex solids content for 2 h to replace the sodium/chloride ions with hydrogen/hydroxyl ions. Afterwards, the surface charge density of the latex particles was determined by conductometric titration. In this procedure, the latex was first diluted to  $\sim 1\%$  solids in a 250 mL beaker and stirred with a magnetic bar. The contents of the beaker were blanketed with inert argon gas to eliminate any contribution from atmospheric  $CO_2$ . The anionic latex was titrated with 0.02N sodium hydroxide and the cationic latex was titrated with 0.02N hydrochloric acid, both at a feed rate of 1.0 mL/min, while recording the conductivity of the latex. Surface charge densities were calculated from the end points of the conductivity curves.

#### Characterization of Cationic and Anionic Particles

Table III presents the diameter and surface charge density of the cationic and anionic latex particles that were used for heteroaggregation. Since the particle size was measured by dynamic light

scattering (DLS, Nicomp), the diameters of the  $M^+$  and  $H^+$  cationic particles represent the water-swollen particle size brought about by the amination. As can be noted, the cationic particle size increased with increasing charge of the particles ( $L^+ < M^+ < H^+$ ). Note that the surface charge density increased to a great extent when the PVBC seed particles ( $L^+$ ) were aminated using trimethylamine (i.e.,  $M^+$  and  $H^+$ ). However, the surface charge density values do not differ widely between  $M^+$  and  $H^+$  despite the 9 $\times$  concentration difference of the amine solution used in the post-polymerization treatment. In addition, the surface charge densities are much lower than the theoretical value ( $\sim 5700 \mu\text{eq/g}$ ). This can be explained by the high concentration of crosslinker (1.33%, Table I) that was used in the synthesis of  $L^+$ . The mechanism for obtaining charge density via amination would be swelling. Namely, trimethylamine did swell the particles and penetrate inside them where chlorine groups exist. Thus, charge density would decrease with increasing crosslinker concentration, since the particles cannot be swollen greatly at high crosslinker concentration. In preliminary experiments, charge densities at different crosslinker concentrations were measured and it was confirmed that the charge density did decrease by increasing the amount of crosslinker that was used. On the other hand, for both anionic particles, the surface charge densities are close to the theoretical values (186 and 441  $\mu\text{eq/g}$  for  $L^-$  and  $H^-$ ). This is evidence that little water-soluble polymer was created in the polymerization, likely owing to the high crosslinker concentrations (2.7% and 2%, Table II).

**Table III.** Particle Size and Surface Charge Density of Latexes Used to Prepare Aggregated Particles

| Latex charge | Latex designation | Particle size ( $D_p$ ) <sup>a</sup> (nm) (PDI) | Charge density ( $\mu\text{eq/g}$ ) |
|--------------|-------------------|---|-------------------------------------|
| Cationic     | $L^+$             | 317 (1.03)                                      | 10                                  |
|              | $M^+$             | 387 (1.06)                                      | 614                                 |
|              | $H^+$             | 466 (1.08)                                      | 860                                 |
| Anionic      | $L^-$             | 42 (2.04)                                       | 185                                 |
|              | $H^-$             | 81 (1.03)                                       | 421                                 |

<sup>a</sup>Intensity-average diameter.

**Table IV.** Amount of Latex and Number Ratio of Anionic ( $H^-$ ) to Cationic Latex Particles ( $H^+$ ) Used to Prepare Heteroaggregated Particles

| Sample designation               | Charge   | Latex (g) | Polymer (g) | Number ratio |
|----------------------------------|----------|-----------|-------------|--------------|
| H <sup>-</sup> H <sup>+</sup> 20 | Anionic  | 2         | 0.02        | 166/1        |
|                                  | Cationic | 2         | 0.01        |              |
| H <sup>-</sup> H <sup>+</sup> 21 | Anionic  | 20        | 0.2         | 1668/1       |
|                                  | Cationic | 2         | 0.01        |              |
| H <sup>-</sup> H <sup>+</sup> 22 | Anionic  | 40        | 0.4         | 3337/1       |
|                                  | Cationic | 2         | 0.01        |              |

### Preparation of Heteroaggregated Particles

Three heteroaggregated latexes were prepared using various combinations of anionic and cationic particles. In a first attempt to obtain heteroaggregated latexes, 0.48 g of L<sup>+</sup> cationic core particles (0.8% solids, Tables I and III), having the lowest surface charge density among the cationic particles, were initially used and added to 0.24 g of the L<sup>-</sup> anionic particle (1.6% solids, Tables II and III) having the lowest charge density. This was done at room temperature under stirring with a magnetic bar at 16 rpm in a 150 mL glass beaker, at a feed rate of 0.5 mL/min using a syringe pump (Harvard Apparatus, Model 22). This method of addition was adopted after it was shown that if the anionic latex was first added to the cationic latex, coagulation resulted owing to what was assumed to be a bridging flocculation mechanism. Thus, this feeding method was used in all subsequent experiments.

Two other combinations of latex particles (H<sup>-</sup>H<sup>+</sup> and H<sup>-</sup>M<sup>+</sup>) were used for preparing other heteroaggregated particles. Cationic particles (H<sup>+</sup>) were added to varying amounts of the anionic particles (H<sup>-</sup>) to study the effect of the anionic-to-cationic particle ratio on the stability (see Table IV).

Finally, heteroaggregated particles were prepared using the intermediate charge density cationic particles (M<sup>+</sup>) and the high surface charge density anionic particles (H<sup>-</sup>). Before the preparation of the heteroaggregated particles, the cationic particles were stabilized by adding 54 g of a 0.9 wt % solution of PVP K30 to 0.25 g of the M<sup>+</sup> particles (0.5% solids; for 1 day in a tumbler at 16 rpm and room temperature). This was done to prevent coagulation that was seen in the preceding experiments. These PVP-stabilized cationic particles were titrated into the anionic particle latex at a feed rate of 0.5 mL/min using the syringe pump, under stirring at 16 rpm with a magnetic bar in a 50 mL glass beaker at room temperature. Table V shows the amounts of cationic and anionic latexes used in preparing a series of heteroaggregated particles that varied in the number ratio of anionic-to-cationic particles.

### Solvent Effect on Heteroaggregation

Studies were carried out to investigate the effect of the solvency of the medium on heteroaggregation using the H<sup>-</sup>M<sup>+</sup>34 aggregated particles (Table V). For this purpose, different concentrations of THF aqueous solutions (10, 20, and 40%) were prepared. Then, 0.048 g of H<sup>-</sup>M<sup>+</sup>34 aggregated particles were added to 24 mL of the THF solutions and tumbled end-over-end at 16 rpm and room temperature for 1 day. The latexes

**Table V.** Amounts of PVP-Stabilized Cationic (M<sup>+</sup>) and Anionic Latexes (H<sup>-</sup>) Used to Form Heteroaggregated Particles at Low Number Ratios

| Sample                           | Cationic latex, g (g of polymer) | Anionic latex, g (g of polymer) | Anionic/Cationic number ratio |
|----------------------------------|----------------------------------|---------------------------------|-------------------------------|
| H <sup>-</sup> M <sup>+</sup> 30 | 16 (0.064)                       | 2 (0.020)                       | 10/1                          |
| H <sup>-</sup> M <sup>+</sup> 31 | 8 (0.032)                        | 2 (0.020)                       | 15/1                          |
| H <sup>-</sup> M <sup>+</sup> 32 | 4 (0.016)                        | 2 (0.020)                       | 31/1                          |
| H <sup>-</sup> M <sup>+</sup> 33 | 2 (0.008)                        | 2 (0.020)                       | 62/1                          |
| H <sup>-</sup> M <sup>+</sup> 34 | 2 (0.008)                        | 4 (0.040)                       | 123/1                         |
| H <sup>-</sup> M <sup>+</sup> 35 | 2 (0.008)                        | 8 (0.080)                       | 246/1                         |

were then centrifuged (10 K rpm, 1 h), the sediment collected and redispersed in 10 mL water, and then sonified for 30 min in an Aquasonic sonifier (VWR Scientific Products, Aquasonic Model 50 T)

## RESULTS AND DISCUSSION

### L<sup>+</sup>L<sup>-</sup> Aggregated Particles

When cationic latex L<sup>+</sup> (Tables I and III) was titrated into anionic latex L<sup>-</sup> (Tables II and III), heteroaggregated particles, referred to as L<sup>+</sup>L<sup>-</sup>, were formed, resulting from the charge attraction of the two particles. A scanning electron microscope image of the particles is shown in Figure 1. The surface charge density of L<sup>+</sup>L<sup>-</sup> is 170  $\mu\text{eq/g}$  based on anionic aggregated particles compared to 185  $\mu\text{eq/g}$  for the anionic particles themselves. However, the conductivity of L<sup>+</sup>L<sup>-</sup> increased with time from 14.2  $\mu\text{S/cm}$  to 22.2  $\mu\text{S/cm}$  after 17 days of storage at room temperature and 93.0  $\mu\text{S/cm}$  after 33 days of storage (0.96% solids content). Two possible explanations for this increase in conductivity are suggested. First, the anionic polystyrene copolymer with sodium styrene sulfonate present could be leached from the particles with time. To confirm this hypothesis, the conductivity and surface charge density of the anionic particles were monitored with time. The results in Table VI show that there was no change in the conductivity of the anionic particles themselves, indicating that leaching out of poly(sodium styrene

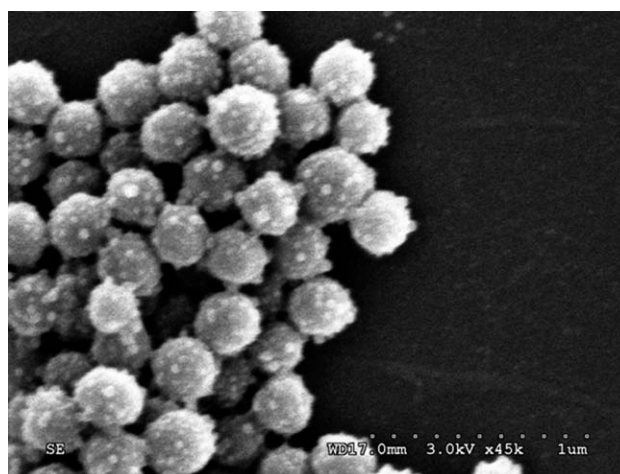


**Figure 1.** SEM image of L<sup>+</sup>L<sup>-</sup> particles prepared by mixing L<sup>+</sup> cationic latex and L<sup>-</sup> anionic latex (Table III).



**Table VI.** Evolution of Surface Charge Density and Conductivity of Anionic Particles ( $L^-$ ) with Time

| Days | Surface charge density ( $\mu\text{eq/g}$ ) | Conductivity ( $\mu\text{S/cm}$ ) |
|------|---|-----------------------------------|
| 0    | $185 \pm 3.3$                               | 390                               |
| 17   | $179 \pm 2.8$                               | 386                               |
| 33   | $173 \pm 0.5$                               | 387                               |

Solids content = 3.7%.

sulfonate) as water-soluble polymer is not the reason for the increase in the conductivity of  $L^+L^-$  with time. The second possible explanation for the increase in conductivity of  $L^+L^-$  is the desorption of the small  $L^-$  anionic particles from the  $L^+L^-$  aggregated particles owing to a relatively weak interaction between the cationic and anionic particles, resulting from the relatively low charge of the two particles. To check this, the initial  $L^+L^-$  particles were filtered using a 200 nm pore size membrane in an effort to remove any small particles in the aqueous phase and the particle size distribution (PSD) was determined by DLS as shown in Figure 2(a) by the gray bars. The PSD after 33 days is shown for comparison by the black bars. The population of small particles increased with time and the large particle population shifted to smaller particle diameters, implying that small particles are being desorbed from the larger cationic particles with time, resulting in changes in the particle size distribution with time. Centrifugation (10 K, 1 h) of  $L^+L^-$  was done as a test of the strength of the attraction between the two particles. Then, the particle size distribution in the sediment layer was measured after centrifugation with results shown in Figure 2(b). The PSD did not change much even after centrifugation, confirming the weak interaction between the core and shell particles.

In an attempt to prevent the desorption of the small anionic particles from the larger cationic particles, the latex was heated in a pressure bottle to  $120^\circ\text{C}$  for 1 day to initiate some coalescence between the core and shell particles. This temperature was above the  $T_g$  of the anionic particles, as measured by DSC ( $105^\circ\text{C}$ ) which is similar to the  $T_g$  of PS ( $100^\circ\text{C}$ ).<sup>43</sup> After heat treatment, however, the conductivity increased from  $6.85 \mu\text{S/cm}$  to  $100 \mu\text{S/cm}$  for the filtered  $L^+L^-$  (0.64% solids) and from  $66 \mu\text{S/cm}$  to  $207 \mu\text{S/cm}$  for the unfiltered  $L^+L^-$  (0.96% solids). The conductivity also continued to increase with time as shown in Figure 3(a). The  $L^+L^-$  latex aged for 6 days, was then subjected to two ion exchange cycles with the conductivities dropping to  $3.89 \mu\text{S/cm}$  and  $9.6 \mu\text{S/cm}$ , respectively. On the basis of these results, it was initially speculated that some of the sulfonated copolymer present in the anionic particles was being leached out at the higher temperature, resulting in an increased conductivity. To test this hypothesis, the anionic latex particles themselves were heated at two different temperatures [ $90^\circ\text{C}$  and  $125^\circ\text{C}$ ; Figure 3(b)], and the conductivity monitored with time. However, the conductivity remained constant, leading us to conclude that the increase in conductivity was instead being caused by the core cationic particles. This was proved by heating the cationic particles [Figure 3(c)] and monitoring their conductivity. The results in Figure 3(c) show a large increase in

conductivity at the elevated temperature, but did not increase over time. This may have something to do with the solids content. The solids content for the latexes shown in Figure 3(a) is less than 1% compared to 32% solids or 10% solids content for the anionic and cationic latex particles shown in Figure 3(b,c), respectively. When the system is diluted, the particle-particle distance is larger than when the latex is concentrated. In addition, the particle mobility, which is one of the factors that affects conductivity, increases in the case of dilution. Namely, conductivity changes are not evident with time for concentrated cationic and anionic latex particles [Figure 3(b,c)] unlike diluted  $L^+L^-$  aggregated particles. Also, heating has another effect in this system. Namely, heating may accelerate desorption of anionic latex particles from the core cationic particles, and thus these anionic particles themselves would result in an increase in conductivity with time as shown in Figure 3(a), since the conductivity change of unfiltered latex particles in Figure 3(a) is higher than filtered particles. The major difference between filtered and unfiltered particles is the presence of free smaller anionic particles that are present in the aqueous phase.

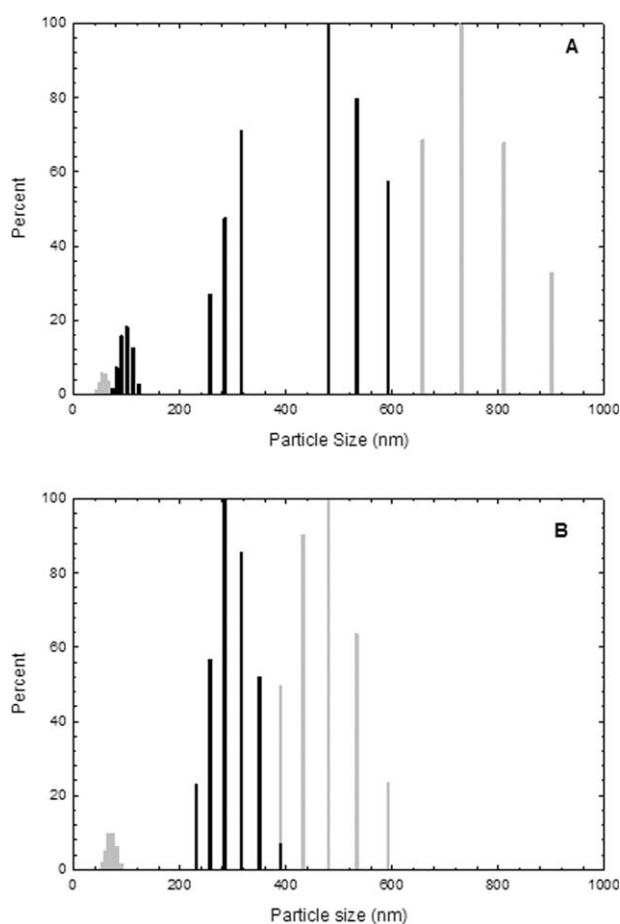


**Figure 2.** (a) Comparison of  $L^+L^-$  particle size distribution (DLS, Nicomp; filtered through 200 nm membranes) (light bars) with the one obtained after 33 days of aging (dark bars), and (b)  $L^+L^-$  particle size distribution before (light bars) and after (dark bars) centrifugation (10 K, 1 h, room temperature).

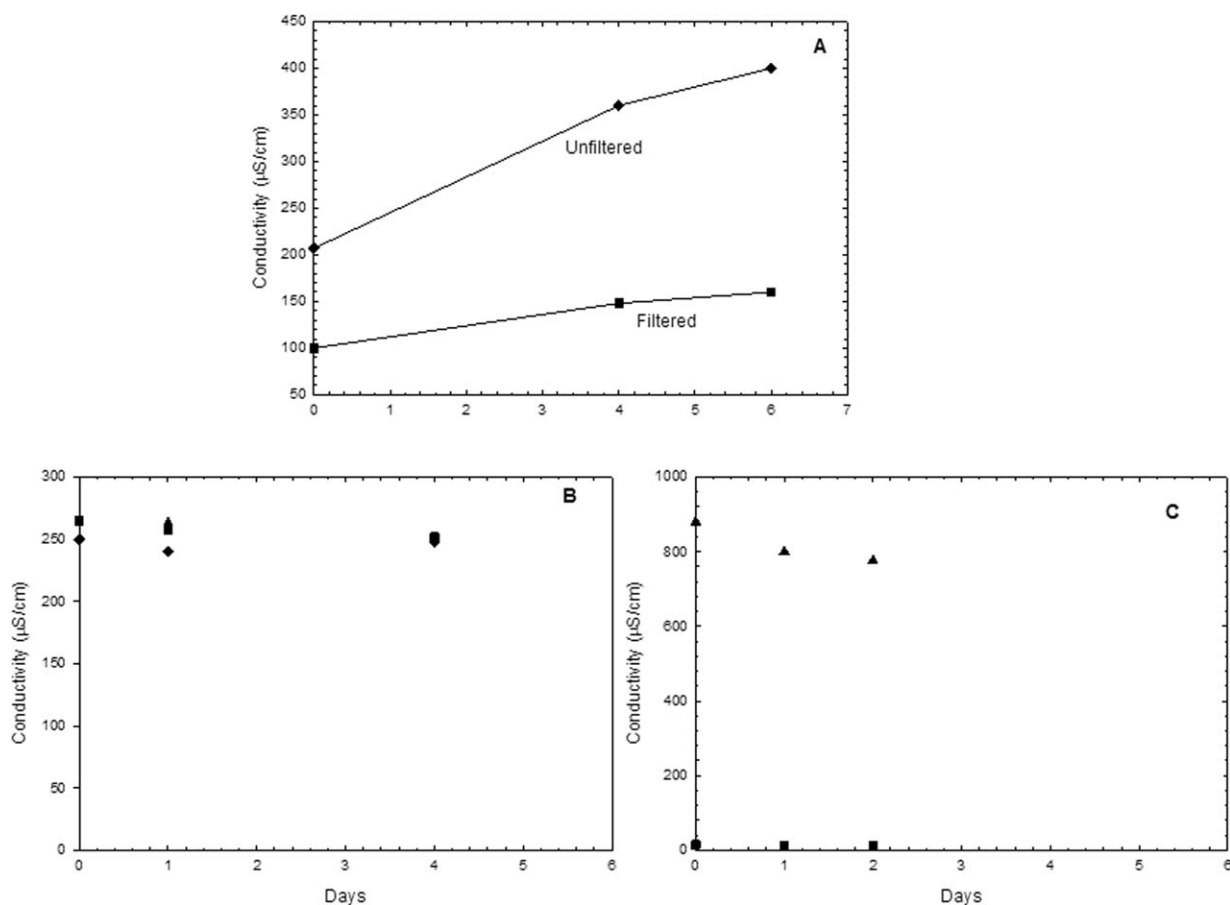


**Figure 3.** (a) Conductivity of unfiltered L<sup>+</sup>L<sup>-</sup> (◆) at 0.96% solids and filtered L<sup>+</sup>L<sup>-</sup> particles (■) at 0.64% solids, as a function of time; (b) conductivity of anionic latex particles at 32% solids (L<sup>-</sup>, Table VI) after heat treatment at different temperatures (◆: 120°C, ■: 90°C, ▲: 25°C) as a function of time; (c) conductivity of cationic latex particles (L<sup>+</sup>, Table VI) at 10% solids after heat treatment at different temperatures (▲: 120°C, ■: 25°C) as a function of time.

### H<sup>+</sup>H<sup>-</sup> Series Aggregated Particles

On the basis of the preceding results, which demonstrated a relatively weak association between the lowest charge pair of particles, heteroaggregations were carried out using the particles with the highest charge densities, namely H<sup>+</sup> and H<sup>-</sup>. A study was carried out to examine the effect of the anionic to cationic particle ratio on the aggregate stability, since coagulum was observed visually when the same amount of cationic latex (2 g, 0.5% solids) was used as anionic latex (2 g, 1% solids) in the heteroaggregation. By increasing the amount of anionic latex (20 g, 1% solids), coagulum was not observed visually but only by SEM imaging [see Figure 4(a,b)]. When 2 g of cationic latex (0.01 g polymer) was added to 40 g of anionic latex (0.4 g polymer), stable aggregated particles (H<sup>+</sup>H<sup>-</sup>22) were obtained [Figure 4(c,d)] as confirmed by scanning electron microscopy where the cationic particles are fully covered by anionic particles. Using a smaller amount of anionic latex for a given amount of cationic latex resulted in coagulum formation because the cationic particles were only partially covered (see Figure 5).

The most stable aggregated particles, namely H<sup>+</sup>H<sup>-</sup>22, were studied further. First, the particle diameter was measured by TEM and compared before and after heteroaggregation. The

core cationic particle diameter was 312 nm, while the aggregated particle size was 420 nm, giving an estimated total number of small particles in the shell layer ( $N_{\text{small}}$ ) of 296 ( $N_{\text{small}} \times V_{\text{small}} = V_{\text{aggregateparticle}} - V_{\text{coreparticle}}$ ). This value of  $N_{\text{small}}$  is slightly higher than  $N_{\text{sat}}$  (247), which is the number of small particles that could be hexagonally close-packed in a monolayer, as given by equation.<sup>44</sup> This indicates that the cationic particles are surrounded by slightly more than a monolayer of anionic particles.

A SEM image of sample H<sup>+</sup>H<sup>-</sup>22 is shown in Figure 6 (right; the core cationic latex is shown on the left) which indicates that agglomeration may have occurred among the H<sup>+</sup>H<sup>-</sup>22 particles. However, this could also be an artifact caused by drying the sample for the SEM analysis. Thus, H<sup>+</sup>H<sup>-</sup>22 was placed in a test tube and the solids content of the top layer was measured after 10 days to allow any settling of agglomerates. Although there was some sediment present at the bottom of the test tube, the solids content of the top layer was 0.85% ± 0.05% out of a total solids content of 0.95%, indicating that the majority of the H<sup>+</sup>H<sup>-</sup>22 particles remained dispersed in the aqueous phase.

The conductivity and surface charge density of H<sup>+</sup>H<sup>-</sup>22 were 98 μS/cm (0.85% solids) and 251 μeq/g (based on anionic particles),

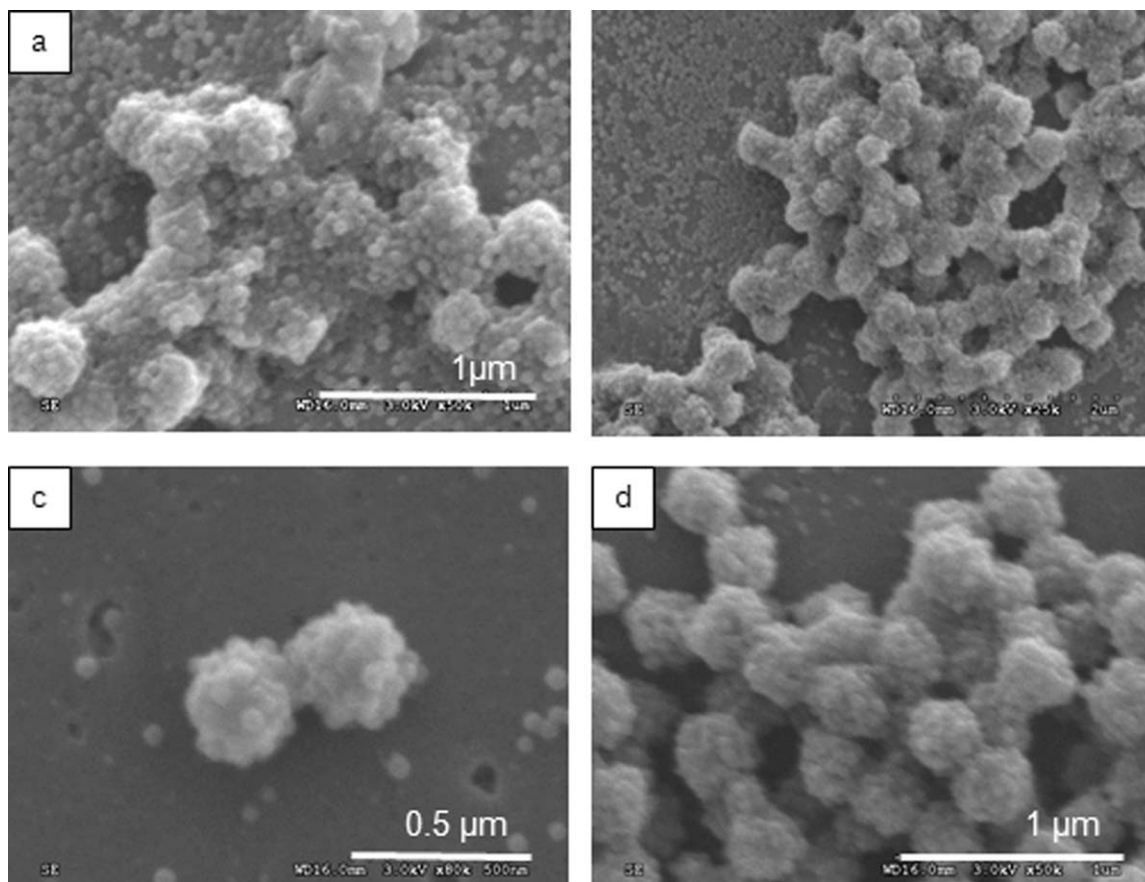


**Figure 4.** (a and b) SEM images of  $H^+H^-21$  particles (number ratio of anionic to cationic particles = 1668) prepared by mixing  $H^+$  cationic latex and  $H^-$  anionic latex under the conditions reported in Table IV; (c and d) SEM images of  $H^+H^-22$  particles (number ratio of anionic to cationic particle = 3337); see Table IV.

respectively, compared to  $265 \mu S/cm$  (1% solids) and  $421 \mu eq/g$  for the anionic particles themselves. Note that the conductivity is still relatively high ( $98 \mu S/cm$  at 0.85% solids). This is likely because of the presence of free small anionic particles in the aqueous phase, estimated to be  $\sim 3000$  per aggregate particle based on the given core and aggregate particle size. Thus, an effort was made to remove any free small particles. Serum replacement, using a series of different pore size membranes (0.4, 0.6, and  $1 \mu m$ ) to filter out particles of different sizes, was tried first. DI water was fed into the serum replacement cell, but coagulum was formed during the process (Figure 7, left). To improve the stability, 1 mM Igepal CO 880 nonionic surfactant solution was fed to the serum replacement cell to provide steric stabilization, but despite this, coagulum still formed (Figure 7, right). It can be seen in the micrographs that coagulation occurred before the small particles were depleted from the latex.

Separation by centrifugation (10,000 rpm, 4 h, room temperature) was tried next. To minimize possible aggregation during the centrifugation, 1 mM or 0.01 mM concentrations of different surfactant solutions (5 mL of Igepal CO 880, PVP K-30, or PVP K-90), were mixed with sample  $H^+H^-22$  (5 g) in glass bottles and mixed by end-over-end rotation at 16 rpm and room temperature for 1 day before centrifugation. After centrifugation, the supernatant was analyzed (see Table VII).

When PVP K 90 (MW = 360,000 g/mol) was used, the amount of solids present in the supernatant was higher than both the theoretical total solids content as well as the theoretical maximum small particles by weight, assuming that all the small particles remained in the supernatant. The sediment was then collected, redispersed in 10 mL deionized water, and sonified for 30 min in an Aquasonic sonifier. Figure 8 shows the  $H^+H^-22$  particles collected from the sediment layer of the centrifuge tube, stabilized with different surfactants. Apparently, the PVP K90 forms bridges between the particles because of its high molecular weight.

Lower molecular weight polymeric surfactant PVP K30 (MW = 40,000 g/mol) and nonionic surfactant Igepal CO 880 (MW = 1540 g/mol) were also tested. Igepal CO 880 and PVP K 30 did not show any significant differences at the same concentration (1 mM), as shown in Figure 8.

High power sonification (Branson sonifier, output 3, duty cycle 60, time = 10 min) was also applied to the sediment layers. As a result, particles stabilized with PVP K30 became well separated, whereas they became aggregated in the presence of Igepal CO 880 (Figure 9). Ottewill and Walker found that latex particles smaller than 250 nm were effectively stabilized with a nonionic surfactant (Note that  $D_w$  of  $H^+H^-22$  = 420 nm by TEM).<sup>45</sup> The

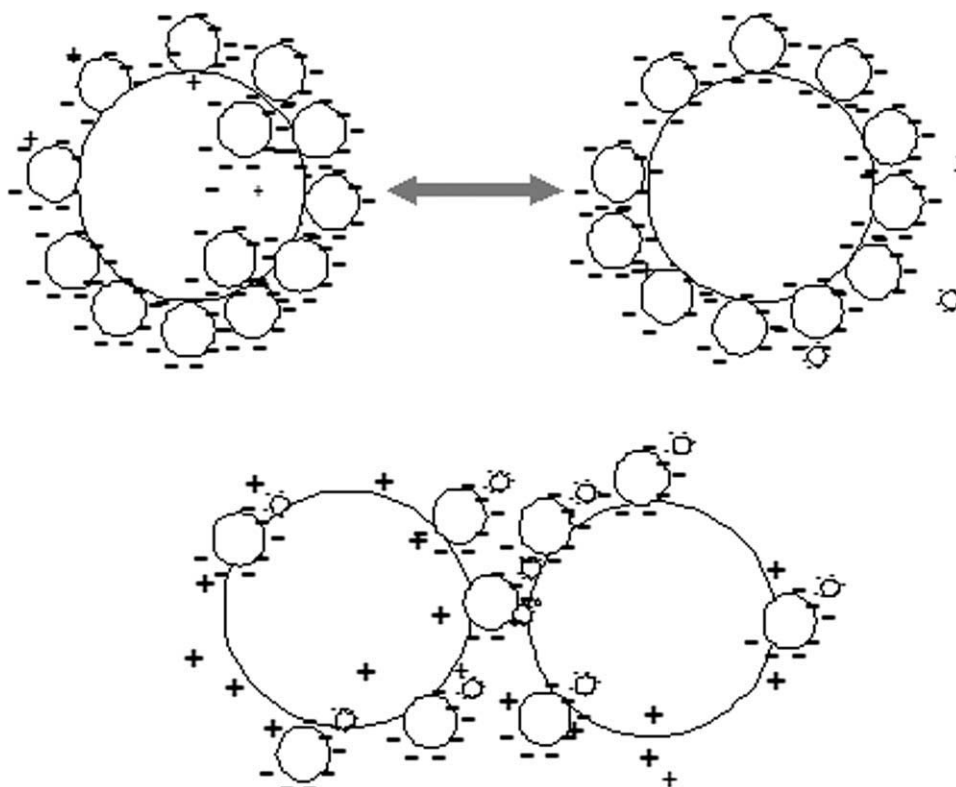


**Figure 5.** Schematic representation of the effect of anionic particle amount on heteroaggregates.

particle diameter was also measured by DLS after each sonification cycle and compared to the core particle size (Table VIII). Although the size of the particles stabilized with PVP K30 decreased each time, the core particle size was not affected by sonification. This suggests that the small particles were not completely removed. In other words, small particles may exist in an aggregated form either adsorbed on the surface of the core particles or among themselves before sonification, affecting the overall particle size decrease with each cycle.

Although two different methods were tried to remove the population of small particles, free small particles were not completely removed in either case. Thus, the next step was to decrease the

number ratio of anionic to cationic particles used in the heteroaggregation. However, using less than 0.4 g of anionic particles, the amount used for  $H^+H^-22$ , caused coagulation. To use less anionic latex, 54 g of a 0.9 wt % solution of PVP K30 stabilizer, which imparted the greatest extent of steric stabilization to the latex in the above experiment, was added to 0.25 g of the  $H^+$  particles (0.5% solids; tumbled at room temperature for 1 day at 16 rpm) in an attempt to reduce the amount of coagulum that may result from the strong attraction of the cationic particles to the anionic particles due to the high cationic charge compared to the low anionic charge. However, coagulation still occurred even when using PVP K30 as stabilizer.

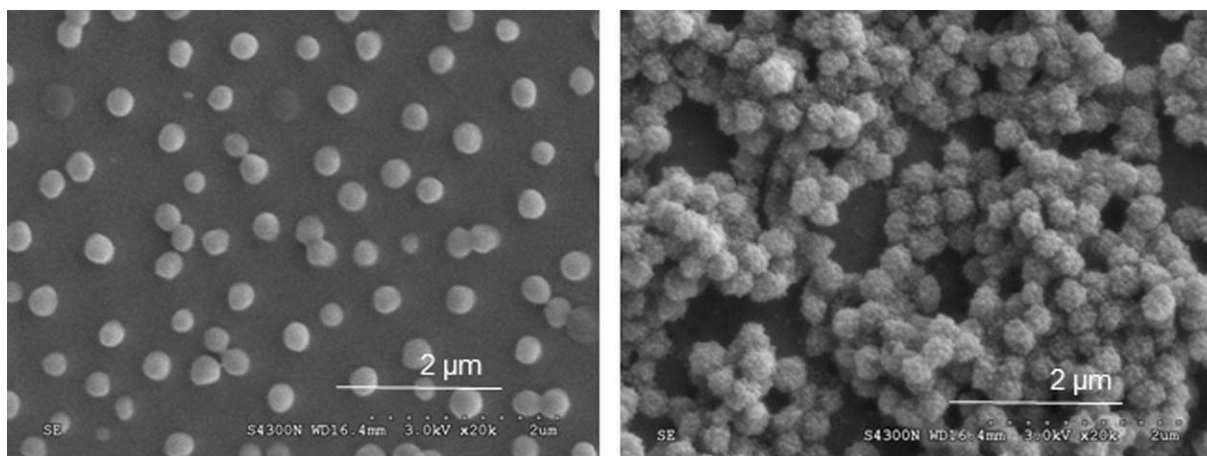


**Figure 6.** SEM images of the cationic core ( $H^+$ , left) and heteroaggregated particles ( $H^+H^-22$ , right).



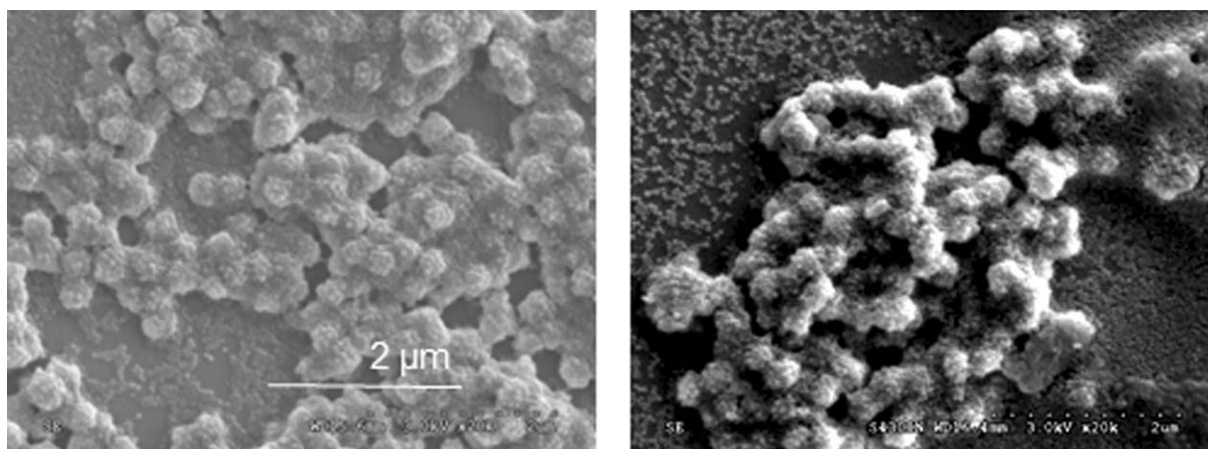


**Figure 7.** SEM images of sample H<sup>+</sup>H<sup>-</sup>22 after serum replacement with DI water (left) and after adding 1 mM Igepal CO 880 surfactant solution (right).

**Table VII.** Supernatant of H<sup>+</sup>H<sup>-</sup>22 Latex Stabilized with Different Stabilizer Solutions after Centrifugation

| Stabilizer <sup>a</sup> | Amount (g)     | % Solids in the supernatant | Theoretical total solids (%) | Theoretical maximum % small particles |
|-------------------------|----------------|-----------------------------|------------------------------|---------------------------------------|
| Igepal CO 880           | 0.01 (1.0 mM)  | 0.3                         | 0.5                          | 0.48                                  |
| PVP K 30                | 0.2 (1.0 mM)   | 2.4                         | 2.45                         | 2.4                                   |
| PVP K 90                | 0.02 (0.01 mM) | 0.9                         | 0.6                          | 0.58                                  |

Centrifugation at 10,000 rpm for 4 h at room temperature.  
<sup>a</sup>5 mL stabilizer.

### M<sup>+</sup>H<sup>-</sup> Series Aggregated Particles

A third combination of cationic and anionic particles was investigated. Aggregated particles were prepared using the cationic particles with an intermediate charge density (M<sup>+</sup>) and the H<sup>-</sup> particles. Before the preparation, PVP K30 was used to stabilize either the cationic or anionic particles, and then heteroaggregation was carried out. It was observed (visually) that the par-

ticles were more stable when the cationic particles were stabilized with PVP K30 compared to either anionic particles or both types of particles. Thus, cationic particles, stabilized with 1 mM PVP K30, were added dropwise into the anionic particle latex to form heteroaggregated particles. Table V presented the amounts of cationic and anionic latexes used in this experiment as well as the number ratio of anionic to cationic

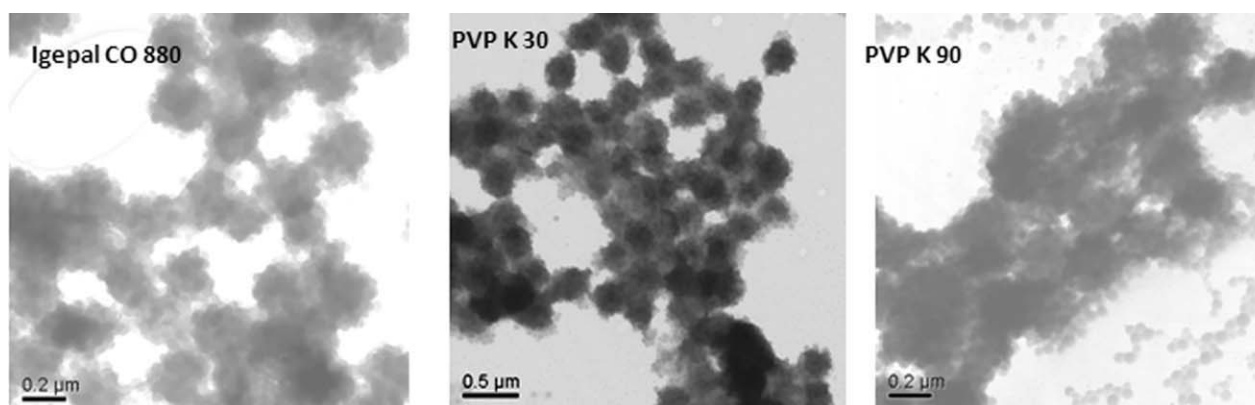


**Figure 8.** SEM images of sample H<sup>+</sup>H<sup>-</sup>22, stabilized with different surfactants (Igepal CO 880, PVP K30, and PVP K90 from left to right) in the sediment after centrifugation.

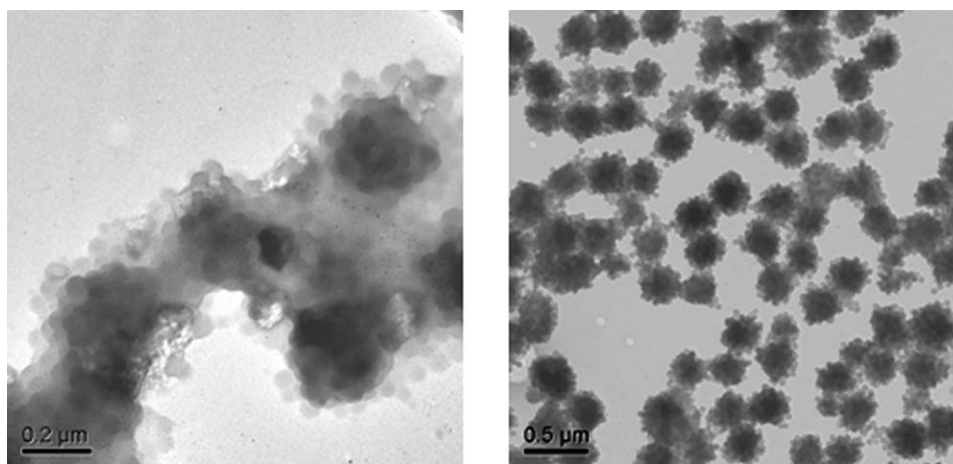


**Figure 9.** SEM images of sample  $H^+H^-22$  after sedimentation and redispersion; Igepal CO 880 (left) and PVP K30 (right; Branson sonifier, output 3, duty cycle 60, time 10 min).

particles. Among these combinations, sample  $M^+H^-34$  was chosen because it produced aggregate particles without coagulation and has a relatively low number ratio of anionic to cationic particles (123), which should result in few free small particles present in the aqueous phase. No coagulum was detected, confirmed by particle size analysis (Nicomp) as reported in Figure 10(a). Also, centrifugation was carried out to test the strength of interaction of the aggregates. Even after one cycle of centrifugation, the particle size did not change unlike the previous  $L^-L^+$  case [Figure 10(b)].

As described previously, THF was used to bring about some coalescence between the particles in an aggregate, thereby creating irreversible attachment. However, the addition of THF had other consequences, facilitating aggregation. Further study on the effect of added THF on heteroaggregation was carried out to determine if more anionic particles could become attached to the cationic core particles. Subsequently, THF was added at concentrations of 10% and 20% (24 mL of THF aqueous solution) to the aggregated latex (0.048 g) characterized in Figure 10. TEM images indicated that an increased number of small anionic particles were attached to the core particles with increasing THF concentration, as shown in Figure 11.

Since this phenomenon could be a result of sample preparation for the TEM, the size of the  $M^+H^-34$  aggregated particles as well as those dispersed in 20% THF were also measured by DLS

(Figure 12). The results indicate that a large number of additional small anionic particles were attached to the core cationic particles. This result can be explained as follows. Solvent further swells the already water-swollen aminated PVBC core particles. Thus, the core particle surface area will be enlarged, allowing more anionic particles to aggregate with the swollen core particles to reduce the total interfacial energy.<sup>46–48</sup> From a kinetic point of view, the presence of solvent can be a factor to enhance the aggregation. Namely, some of the PVP K30 stabilizer

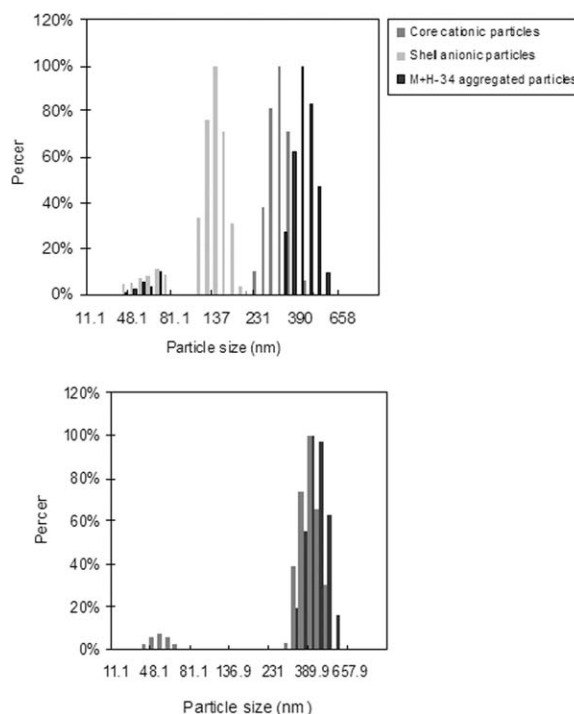


**Figure 10.** (a)  $M^+H^-34$  heteroaggregated particle size distribution compared to cationic core particles ( $M^+$ ) and shell anionic particles ( $H^-$ ; DLS, Nicomp); (b)  $M^+H^-34$  particle size before (light bars) and after (dark bars) centrifugation (10 K, 1 h).

**Table VIII.** Comparison of  $H^+H^-22$  in the Sediment Layer with Core Particle ( $H^+$ ) Size after Several Ultrasonification Cycles

| Sample                              | $D_1$ (nm)           | $D_1$ (nm)             | $D_1$ (nm)                |
|-------------------------------------|----------------------|------------------------|---------------------------|
|                                     | Without sonification | One cycle <sup>a</sup> | Second cycle <sup>a</sup> |
| $H^+H^-22$ stabilized with PVP K-30 | 693.6                | 422.3                  | 376.7                     |
| Core particle (nm)                  | 466.7                | 465.8                  | 467.7                     |

<sup>a</sup>Branson sonifier, output 3, duty cycle 60, time 10 min.

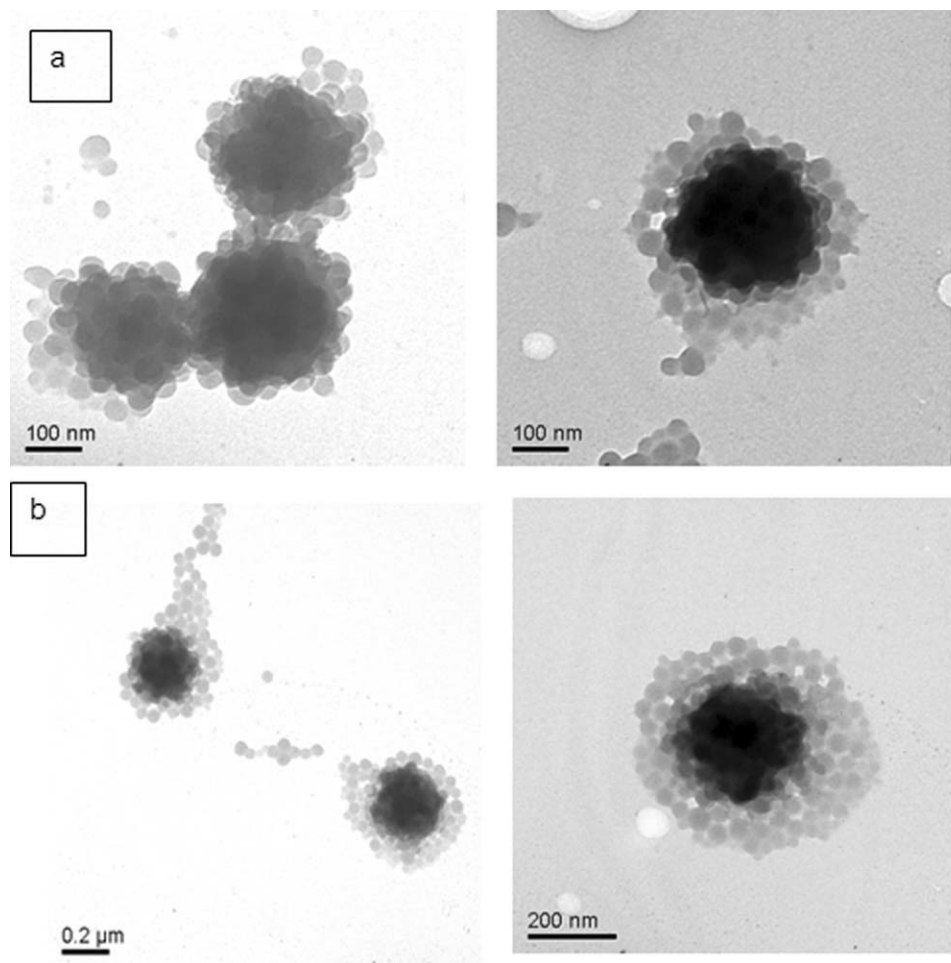


**Figure 11.** TEM micrographs of  $M^+H^-34$  aggregated particles treated with (a) 10% THF in the aqueous phase and (b) 20% THF in the aqueous phase.

attached to the core particles can be desorbed by adding solvent to the aqueous phase, facilitating aggregation.

## CONCLUSIONS

Three different aggregate particles ( $L^+L^-$ ,  $H^+H^-$ , and  $M^+H^-$ ) were prepared by heteroaggregating combinations of large-size cationic particle having low ( $L^+$ ), medium ( $M^+$ ), and high ( $H^+$ ) charge with small-size anionic particles having low ( $L^-$ ) and high ( $H^-$ ) charge. The  $L^+L^-$  aggregate particles prepared from the low charge cationic ( $L^+$ ) and anionic ( $L^-$ ) latexes proved to have a relatively weak attraction between the core cationic particles and the shell anionic particles, thereby, some of the small particles were desorbed with time. Post heat treatment was carried out to fuse the anionic particles onto the surface of the cationic particles, but this led to an increase in conductivity owing to ions leaching from the cationic particles at high temperature. The  $H^+H^-22$  particles, prepared by adding the high charge cationic ( $H^+$ ) to the high charge anionic particles ( $H^-$ ), were shown to have the cationic particles fully covered by the anionic particles and it was confirmed that there was more than a single layer of the shell anionic particles. However, because a relatively large ratio of the anionic to cationic particles proved necessary to create a stable heteroaggregation structure, there

were many free small anionic particles present in the aqueous phase, which resulted in increased conductivity and the necessity of their removal. Efforts were made to remove these particles by serum replacement using different pore size membranes (0.4, 0.6, and 1  $\mu\text{m}$ ) in conjunction with centrifugation;

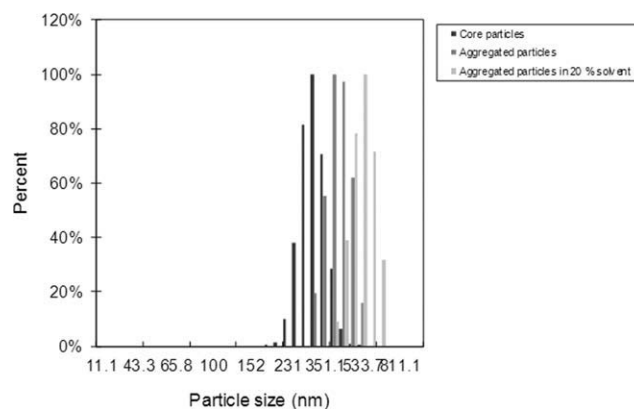


**Figure 12.** Comparison of particle size distributions of cationic core particles,  $M^+H^-34$  aggregated particles, and  $M^+H^-34$  particles treated with 20% THF (DLS, Nicomp).

however, these attempts did not achieve any satisfactory results. Finally,  $M^+H^-34$  was prepared, which represents an intermediate between the two previous cases, that used the medium charge cationic ( $M^+$ ) particles and the high charge anionic ( $H^-$ ) particles. The interaction between the core cationic particles and shell anionic particles was stronger than in  $L^+L^-$ , and there were fewer free anionic particles present in the aqueous phase. In addition, the use of a solvent (THF) treatment enhanced the attachment of more anionic particles to the cationic core particle.

#### ACKNOWLEDGMENTS

Funding for this project by the Department of Energy (DOE; Grant # DE-FG02-04ER83884) and Dynalene, Inc. is gratefully acknowledged.

#### REFERENCES

- Wexler, A. U.S. Pat. 6,297,296 (2001).
- Alinec, B.; Arnoldova, P.; Frolik, R. *J. Appl. Polym. Sci.* **2000**, *76*, 1677.
- Ibba, M.; Stathopoulos, C.; Soll, D. *Curr. Biol.* **2011**, *11*, R563.
- Shinkai, M. *J. Biosci. Bioeng.* **2002**, *94*, 606.
- Kim, J. H.; El-Aasser, M. S.; Klein, A.; Vanderhoff, J. W. *J. Appl. Polym. Sci.* **1988**, *35*, 2117.
- Govedarica, M. N.; Dvornic, P. R. *J. Serb. Chem. Soc.* **1991**, *56*, 7.
- De Lucas, A.; Canizares, P.; Rodriguez, J. F. *Separ. Sci. Technol.* **1995**, *30*, 125.
- Djinovic, V. M.; Antic, V. V.; Djonlagic, J.; Govedarica, M. N. *React. Funct. Polym.* **2000**, *44*, 299.
- Malini, K. A.; Anantharaman, M. R.; Sindhu, S.; Chinnasamy, C. N.; Ponpandian, N.; Narayanasamy, A.; Balachandran, M.; Pillai, V. N. S. *J. Mater. Sci.* **2011**, *36*, 821.
- Jingu, N.; Satoh, M.; Kitamura, K.; Yoshimura, M. U.S. Pat. Appl. Publ. #20090136783 (2009).
- Tran, N.; Pareta, R.; Webster, T. J. Materials Research Society Symposium Proceedings, 1136E (Materials in Tissue Engineering), Paper #: 1140-HH06-20-DD03-20 (2009).
- Gupta, A. K.; Gupta, M. *Drug Deliv.* **2008**, *1*, 205.
- Guimaraes, A. R.; Rakhlin, E.; Elena, R.; Weissleder, S. P. *Thayer Pancreas* **2008**, *37*, 440.
- Pawelczyk, E.; Jordan, E. K.; Balakumaran, A.; Chaudhry, N.; Gormley, N.; Smith, M.; Lewis, B. K.; Childs, R.; Robey, P. G.; Frank, J. A. *PLoS One* **2009**, *4*.
- Yang, L.; Cao, Z.; Sajja, H. K.; Mao, H.; Wang, L.; Geng, H.; Jiang, T.; Wood, W. C.; Nie, S.; Shuming, J. *Biomed. Nanotechnol.* **2008**, *4*, 439.
- Peng, X.; Qian, X.; Mao, H.; Wang, A. Y.; Chen, Z.; Nie, S.; Shin, D. M. *Int. J. Nanomed.* **2008**, *3*, 311.
- Kim, D. K. *J. Magn. Magn. Mater.* **2001**, *225*, 256.
- Esenaliev, R. O. U.S. Pat. 6,165,440 (2000).
- Gray, B. N.; Jones, S. K. U.S. Pat. 6,167,313 (2000).
- Jordan, A. J. *Magn. Magn. Mater.* **1999**, *201*, 413.
- Chen, N.; Hong, L. *Solid State Ionics* **2002**, *146*, 377.
- Chen, S.; Krishnan, L.; Srinivasan, S.; Benziger, J.; Bocarsly, A. B. *J. Membr. Sci.* **2004**, *243*, 327.
- Oren, Y.; Freger, V.; Linder, C. J. *Membr. Sci.* **2004**, *239*, 17.
- Yeager, A. S. H. L. *J. Electrochem. Soc.* **1981**, *128*, 1880.
- Floria, V. D. Dow Chemical Co., U.S. Pat. 2,971,935 (1961).
- Juang, M. S.; Krieger, I. M. *J. Polym. Sci. Polym. Chem. Ed.* **1976**, *14*, 2089.
- Kim, J. H. Ph.D. Dissertation, Lehigh University (1986).
- Turner, S. R.; Weiss, R. A.; Lundberg, R. D. *J. Polym. Sci. Polym. Chem. Ed.* **1985**, *23*, 535.
- Grosse, C.; Pedrosa, S.; Shilov, V. N. *J. Colloid Interface Sci.* **2002**, *251*, 304.
- Hen, J. J. *J. Colloid Interface Sci.* **1974**, *49*, 425.
- Luckham, P. F.; Vincent, B.; Hart, C. A.; Tadros, Th. F. *Colloids Surf.* **1980**, *1*, 281.
- Ottewill, R. H.; Schofield, A. B.; Waters, J. A.; Williams, N. S. *J. Colloid Polym. Sci.* **1997**, *275*, 274.
- Kim, A. Y.; Berg, J. C. *J. Colloid Interface Sci.* **2000**, *229*, 607.
- Fernandez-Barbero, A.; Vincent, B. *Phys. Rev.* **2001**, *E 63*.
- Puertas, A. M.; Fernandez-Barbero, A.; de las Nieves, F. J. *J. Chem. Phys.* **2011**, *115*, 5662.
- Yates-George, P. D.; Franks, V.; Jameson, G. J. *Colloids Surf. A: Physicochem. Eng. Asp.* **2008**, *326*, 83.
- Yates-George, P. D.; Franks, V.; Jameson, G. J. *Colloids Surf. A: Physicochem. Eng. Asp.* **2008**, *326*, 83.
- Li, H.; Han, J.; Panioukhine, A.; Kumacheva, E. *J. Colloid Interface Sci.* **2002**, *225*, 119.
- Guoliang, L.; Xinlin, Y.; Junyou, W. *Colloid Surf. A* **2008**, *322*, 192.
- Guoliang, L.; Yanyan, S.; Xinlin, Y.; Wenqiang, H. *J. Appl. Polym. Sci.* **2007**, *104*, 1350.
- Li, R.; Yang, X.; Li, G.; Li, S.; Wenqiang Huang, W. *Langmuir* **2006**, *22*, 8127.
- Ahmed, S. M.; El-Aasser, M. S.; Pauli, G. H.; Poehlein, G. W.; Vanderhoff, J. W. *J. Colloid Interface Sci.* **1980**, *73*, 388.
- Montheard, J. P.; Camps, M.; Kawaye, S.; Pham, Q. T.; Seytre, G. *Makromol. Chem.* **1982**, *183*, 1191.
- Ottewill, R. H. In Emulsion Polymerization and Emulsion Polymers; El-Aasser, M. S., Lovell, P. A., Eds.; John Wiley and Sons: Chichester, England, **1997**.
- Ottewill, R. H.; Walker, T. *JCS Faraday I* **1974**, *70*, 917.
- Ottewill, R. H.; Schofield, A. B.; Waters, J. A. *Colloid Polym. Sci.* **1996**, *274*, 763.
- Waters, J. A. U.S. Pat. 5,210,113 (1990).
- Waters, J. A. U.S. Pat. 5,296,524 (1993).